Available online at www.sciencedirect.com
ScienceDirect
Ceramics International 37 (2011) 2237–2245
CERAMICS INTERNATIONAL
www.elsevier.com/locate/ceramint

Fabrication of magnesium aluminate ($MgAl_2O_4$) spinel foams

Ibram Ganesh

Centre for Advanced Ceramics, International Advanced Research Centre for Powder Metallurgy and New Materials (ARCI), Hyderabad 500 005, A.P., India

Received 3 May 2010; received in revised form 5 February 2011; accepted 7 March 2011
Available online 14 April 2011

Abstract

This paper reports on a novel-processing route for fabricating magnesium aluminate ($MgAl_2O_4$) spinel (MAS) foams from aqueous suspensions containing 30–35 vol.% solids loading. A stoichiometric MAS powder formed from alumina (71.8%) and magnesia (28.2%) at 1400 °C was surface passivated against hydrolysis in an ethanol solution of H_3PO_4 and $Al(H_2PO_4)_3$ at 80 °C for 24 h. Stable aqueous suspensions with 30–35 vol.% solids loading were prepared using the surface passivated MAS powder with the help of tetra-methylammonium hydroxide (TMAH) and an ammonium salt of polyacrylic acid (Duramax D-3005) employed as dispersing agents. An aqueous solution of N-cetyl-N,N,N-trimethy-lammonium bromide (CTMAB) was utilized to create foam in aqueous MAS suspensions by mechanical frothing. Liquid foam was then consolidated in non-porous moulds by introducing a polymerization initiator and a catalyst under ambient conditions. Dried (at >90 °C for 24 h) MAS foams were then sintered for 1 h at 1650 °C. For comparison purposes, dense MAS bodies out of an un-passivated stoichiometric MAS powder, and, dense as well as foams out of alumina were also prepared in this study. The sintered properties of MAS and alumina ceramics were characterized by various means and thus obtained results are presented and discussed in this paper. The sintered MAS foams exhibited a porosity of about 74–76% and a compressive strength of about 4–7.2 MPa inline to values reported for other ceramic foams in the literature.

Keywords: $MgAl_2O_4$ spinel; Foams; Gelcasting; Surface passivation; Compressive strength

1. Introduction

Recently, ceramic foams have gained a great deal of importance for certain applications such as, filters, membranes, sensors, catalyst carriers, piezoelectric ceramics, biomedical and construction materials [1–8]. Several fabrication routes such as, burning out a polymeric sponge impregnated with a ceramic suspension [2], solid-state sintering [3], sol–gel process [4], replication of polymer foams by impregnation [5], aqueous gelcasting [6–8], etc., have been developed to prepare these ceramic foams. Among these routes, the aqueous gelcasting was found to be an easy and most attractive process to prepare ceramic foams with relatively higher porosity [9]. Aqueous gelcasting combines the foaming of aqueous suspension of ceramic powder and organic monomers and the *in situ* polymerization of the foamed suspension. The foaming in the ceramic suspension is accomplished by addition of surfactant (i.e., a foaming agent) followed by mechanical mixing. A surfactant is necessary for the stabilization of the generated liquid foam for a longer time prior to solidification by reducing the surface tension of the gas–liquid interfaces. In fact, the final strength of the sintered foam is strongly dependant of the degree of densification achieved in the foam webs upon sintering. It has been reported that the densification behaviour of powder particles in compacts consolidated following colloidal processing routes is strongly influenced by the degree of compactness achieved in the green body and by the effective de-agglomeration of the powder particles in the suspension during ball milling operation [10–17]. So far, Al_2O_3 [1,12–15], PZT [4], SiC [16], alumino-silicate [17], etc., foams have been prepared following either aqueous gelcasting or other colloidal processing routes.

Recently, MAS has been identified as one of the technologically important materials and was employed in several applications owing to its many attractive properties such as, high melting point (2135 °C), high hardness (16.1 GPa), relatively low density (3.58 g/cm^3), excellent transmittance in the wavelength range of 0.25 μm to 5.0 μm, high strength (180 MPa) at room and at elevated temperatures, high chemical inertness, relatively low thermal expansion coefficient (9×10^{-6}/°C between 30 and 1400 °C) and high thermal

E-mail addresses: ibramganesh@arci.res.in, ibram_ganesh@yahoo.com.

0272-8842/$36.00
doi:10.1016/j.ceramint.2011.03.068

shock resistance [18,19], etc. Furthermore, MAS does not react with SiO_2 until 1735 °C, with MgO or CaO until 2000 °C, with Al_2O_3 until 1925 °C and it can be in contact with all metals except alkaline earths [19]. On account of these attractive properties, MAS has been employed for optical windows for pressure vessels and bullet proof vehicles [20], alternative materials to replace the conventional carbon anode in aluminium electrolytic cells [21], humidity sensors [22], refractory materials for cement rotary kilns and steel ladles [23–25] and as catalyst support for several commercially important reactions [26,27]. However, ceramic foams out of MAS have not been prepared so far despite its high temperature withstanding capability and high temperature strength. There could be primarily two reasons for not preparing MAS foams so far. The first one is its high manufacturing cost and the second one is its high basic nature. The considerable amount (~8%) of volume expansion associated with MAS phase formation from alumina and magnesia upon firing does not allow forming dense MAS bodies in a single-stage reaction sintering (firing) process [28–30]. In order to overcome this problem, the alumina and magnesia raw materials mixtures are normally calcined at around 1500 °C to obtain powders with >80% MAS phase, and then regrinding the calcined powder, re-compaction and re-firing at >1650 °C to obtain dense bodies (i.e., a double-stage firing process) [29,30]. Due to the involvement of two consecutive firing cycles, the cost of production of MAS ceramics has been increased considerably. Due to its high basic nature, MAS powder reacts with water during processing thereby makes aqueous colloidal processing cumbersome [22,31].

This paper reports a simple way to prepare MAS foams. A stoichiometric MAS powder formed from alumina and magnesia powders at 1400 °C was passivated against hydrolysis [32] and then dispersed in aqueous medium to obtain stable suspensions with solids loading in the range of 30–35 vol.% [33]. These stable suspensions were converted into liquid foam with the help of CTMAB. This stable liquid foam was then cast in non-porous moulds following gelcasting route, dried and sintered for 1 h at 1650 °C. For comparison purposes, dense as well as foam bodies out of a commercially available alumina powder and dense MAS bodies out of an un-treated stoichiometric MAS powder were consolidated following either aqueous gelcasting route or a conventional dry-powder pressing route, and then sintered at temperatures in the range of 1600–1650 °C for 1–2 h and characterized them for various properties. Thus obtained results are presented and discussed in this paper.

2. Experimental procedure

2.1. Synthesis of MAS powder

A stoichiometric mixture of alumina (CT-3000SG, Alcoa-Chemie GmbH, Ludwigshafen, Germany, average particle size = 1.84 μm, BET SSA ~ 4 m^2/g, consisting of corundum phase, ICDD File No.: 00-46-1212) and calcined caustic magnesia (José M. Vaz Pereira, S.A., Porto, Portugal, average particle/agglomerate size = 5.63 μm, BET SSA ~15 m^2/g, consisting of periclase phase, ICDD File No.: 00-45-946, the weight ratio of $CaO/SiO_2 = 0.936$) was dispersed in an azeotropic mixture of 60 vol.% methyl ethyl ketone (MEK) (Honeywell, Riedel-de Haen, Hanover, Germany) and 40 vol.% absolute ethanol (E) (Merck, Darmstadt, Germany) with the help of Hypermer KD1 (a polyester/polyamine copolymer having an estimated MW of about 10,000 g/mol, Imperial Chemical Industries PLC, London, UK) to obtain a slurry with about 40 vol.% solids loading [34]. The resultant slurry was de-agglomerated for 24 h in a polypropylene bottle using alumina balls and a powder to balls weight ratio of 1:3. The homogenized suspension was separated from the alumina balls and then transferred to a glass beaker and placed in a refrigerator (Whirlpool 310 Deluxe, Whirlpool, Madrid, Spain) at −5 °C to promote consolidation by temperature induced gelation (TIG) in order to preserve in the green cake the homogeneity achieved in the slurry [34]. The consolidated cake was evacuated at a pressure of 1×10^{-1} torr using a vacuum pump (98.93 liters per minute capacity, Model: 949-9315, Varian DS-102; Torino, Italy) at −5 °C and was further dried at about 40 °C in an electric hot-air oven. The gelation mechanism involved in this process was mainly based on the cooling up of dissolved dispersant molecules, inducing *in situ* gelation (i.e., TIG) and the formation of a rigid network bridging the suspended particles [34]. The dried cake was then calcined in an electrically heated open-air muffle furnace for 1 h at 1400 °C to obtain MAS powder. This calcined powder was crushed, ground in a hammer mill (Retsch GmbH, model SK1, Haan, Germany) and then planetary ball milled (Retsch GmbH, PM400, Haan, Germany) at 200 rpm for 3 h in an absolute ethanol. The solids loading in the suspension maintained during ball milling was 30 vol.% and the powder to balls weight ratio of 1:3. Hereafter, the calcined and ground powder is referred to as A-MAS powder.

2.2. Surface passivation of MAS powder

The ground A-MAS powder was passivated against hydrolysis according to a surface treatment procedure developed in author's laboratory [32,33]. In a typical experiment, 245 g of A-MAS was suspended in an absolute ethanol to obtain 250 mL of a 30 vol.% suspension in a 500 mL volume three-neck round-bottom (RB) flask. The RB flask was fitted with an equalization funnel and a valve to pass dry nitrogen gas, and was placed into a thermostatic oil bath (150 mm diameter and 80 mm height Pyrex glass dish, Thermol-100, Biolabs, Hyderabad, India, −50 to +250 °C). In a separate experiment, 2 g of aluminium di-hydrogen phosphate, $Al(H_2PO_4)_3$ (assay ≥ 97.0%, Fluka, Seelze, Germany) was digested in 5 mL of hot ortho-phosphoric acid, H_3PO_4 (85% assay, AR grade, Qualigens, Mumbai, India). This solution was then mixed with 50 mL of ethanol and added drop-by-drop to the above alcohol based MAS suspension with the help of an equalization funnel. The RB contents were then refluxed for 24 h under a N_2 flow rate of 100 mL/min and magnetic stirring (5MLH-DX, Remi, India). The treated MAS

suspension was filtered off and washed with fresh ethanol several times in order to remove the excess of H_3PO_4 and $Al(H_2PO_4)_3$ not bound to the powders' surface. Henceforth, the treated and washed powder is termed T-MAS [35].

2.3. Consolidation of porous and dense ceramics

For making MAS and α-Al_2O_3 foams by gelcasting (GC) route, homogenous suspensions with 30–40 vol.% solids loading were prepared by dispersing the either T-MAS powder or α-Al_2O_3 powder (CT-3000SG, Alcoa-Chemie GmbH, Ludwigshafen, Germany) in an aqueous-organic premix solution obtained by dissolving 20 wt.% MAM (methacrylamide), MBAM (mithylenebisacrylamide) and NVP (n-vinylpyrrolidinone) in 3:1:3 ratio in de-ionized water [36] in the presence of either a mixture of as received 25% aqueous TMAH (Fluka, Seelze, Germany) and Duramax D-3005 (Rohm and Haas, Lauterbourg, France), added at the ratios of 35 μL and 30 μL per gram of powder, respectively, or an aqueous solution of a polycarboxylic acid without alkalis, Dolapix CE 64 (Zschimmer and Schwarz, Chemnitztalstrasse, Germany), added at the ratio of 0.4 wt.% on the dry powder weight basis [33,35]. The dispersed powders were de-agglomerated by ball milling for 24 h in polypropylene bottles using alumina balls with the charge to balls weight ratio of 1:3. The as obtained slurries were sieved (through 150 BSS mesh) and then degassed for 5 min by vacuum pumping. To these stable slurries, a 10 wt.% aqueous solution of CTMAB [$C_{19}H_{42}BrN$, Loba-Chimie, GR Grade, Mumbai, India], an organic foaming agent, at the ratio of 10 μL per gram of slurry was added and performed the milling operation in polypropylene bottles for 24 h using same alumina balls with same weight ratio to generate foam in the slurries [32]. The resultant liquid foams were transferred to plastic beakers and separated alumina balls. A polymerisation initiator (10 wt.% aqueous ammonium persulfate (APS)) and a catalyst (as received tetramethylethylenediammine (TEMED) (both are AR Grade, Qualigens, Mumbai, India)) at the ratio of 4 and 2 μL per gram of foam, respectively, were introduced and stirred for 3 min using a high dense polypropylene rod (12 mm diameter). Casting was performed in non-porous white petroleum jelly coated split type aluminium/plastic moulds [32]. Gelling process was performed under ambient conditions. Green foams thus made were dried under 90% RH conditions at 40 °C for 24 h followed by at 90 °C for another 24 h.

For making solid MAS and alumina bodies, A-MAS and α-Al_2O_3 (CT-3000SG, Alcoa-Chemie GmbH, Ludwigshafen, Germany) powders were converted into granules (−30 to +100 BSS mesh size) following a conventional granules making process, and then dried and compacted in a metal die uniaxially under a pressure of 200 MPa [37,38]. These compacted pellets along with dried foams were heat treated at a rate of 1 °C/min up to 500 °C and held at this temperature for 2 h. Then the sintering was conducted at a heating rate of 5 °C/min up to 1600–1650 °C with 1–2 h holding time at this temperature.

2.4. Material characterization

BET surface areas of the powders were determined by nitrogen physisorption at −196 °C using a Gemini Micromeritics analyzer (Model 2360, Micromeritics, Norcross, GA, Section 2) and assuming a cross section area of N_2 molecule as 0.162 nm^2. Particle size distributions of powders were measured using a particle size analyzer (Coulter LS230, Buckinghamshire, UK). The viscosity of slurries was measured using a rotational Rheometer (Bohlin C-VOR Instruments, Worcestershire, UK). The measuring configuration adopted was a cone and plate (4°, 40 mm, and gap of 150 μm), and flow measurements were conducted between 0.1 and 800 s^{-1}. In addition to this, the absolute viscosities of alumina slurries were also measured on a piston-type viscometer (Viscolab 4100, Cambridge Applied Systems Inc., Boston, MA) to understand variations in the viscosity of the suspension as a function of time under constant shear rate [16]. XRD patterns were recorded on a Rigaku advanced system (Rigaku, Tokyo, Japan) using diffracted beam mono-chromated Cu K_α (0.15406 nm) radiation source. Crystalline phases were identified by comparison with PDF-4 reference data from International Centre for Diffraction Data (ICDD) [39]. To obtain quantitative information of various phases, the most intense peak of the individual phases was taken into consideration. The peak heights of all the phases were summed up and the percentage concentration of a particular phase was estimated from the ratio of the strongest peak of that phase to the sum of various phases present in a given system [39]. Microstructures of densified MAS and alumina ceramics were examined after polishing and etching in boiling H_3PO_4 solution for 5 min by SEM on Hitachi S-4100 equipment (Tokyo, Japan). Bulk density, apparent porosity, and water absorption capacity of sintered samples were measured according to Archimedes principle (ASTM C372) using Mettler balance (AG 245, Mettler Toledo, Heuwinkelstrasse, Switzerland) [29,30]. For each sample, three measurements of bulk density, apparent porosity and water absorption capacity were performed and the results presented are the average (±0.01 error). The crushing strength of sintered foams was measured on a universal testing machine (Instron, UK). The strain rate was maintained as 1.66×10^{-3} s^{-1} during the tests.

3. Results and discussion

The X-ray diffraction pattern of MAS powder formed by the calcination of a stoichiometric mixture of alumina and magnesia at 1400 °C for 1 h after compacting by following the temperature induced gelation (TIG) route is presented in Fig. 1. For the sake of easy comparison, the XRD patterns reported in ICDD files for corundum (ICDD File No.: 00-46-1212), periclase (ICDD File No.: 00-45-946) and for stoichiometric $MgAl_2O_4$ spinel (ICDD File No.: 00-21-1152) are also presented in this figure. It can be seen that the calcined powder exhibits XRD peaks mainly due to MAS phase together with minor peaks due to un-reacted corundum and periclase phases. About 98.1% MAS phase was measured in this calcined

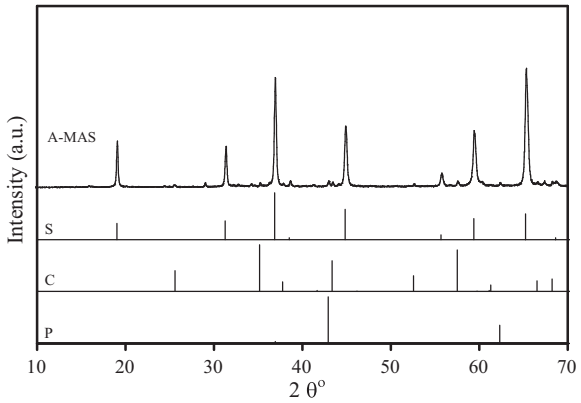

Fig. 1. XRD pattern of a stoichiometric $MgAl_2O_4$ spinel (MAS) powder formed upon calcination of a mixture of alumina and magnesia powders after compacting by following temperature induced gelation (TIG) process for 1 h at 1400 °C. P, periclase, ICDD File No.: 00-45-946; C, corundum, ICDD File No.: 00-46-1212; S, spinel, ICDD File No.: 00-21-1152.

powder. The median particle size and BET surface area of A-MAS powder were estimated to be about 1.91 μm and 3.88 m^2/g, respectively. Good properties were reported for MAS powder having a MAS phase content of about 85%, a median particle size of about 3 μm, and a compact (green) density of >55% of the theoretical density (TD) when sintered at 1650 °C for 1 h [29,30]. Otherwise, the volume expansion (∼8%) associated with the MAS phase formation from alumina and magnesia does not allow forming a dense body upon sintering [28]. It has been reported that the partially spinelized (∼90%) powders possess higher reactivity during sintering in comparison with fully spinelized or un-calcined powder at elevated temperatures [37]. This is mainly because of requirement of higher calcination temperatures for complete spinelization compared to partial spinelization leading to the formation of hard agglomerates of the powders, which in turn results in lowering the reactivity of powders. Keeping these facts in the mind, purposefully, the calcination temperature was restricted only to 1400 °C for 1 h to retain some small amounts of un-reacted alumina and magnesia in the calcined powder, which would react during sintering thereby promoting the densification process [37,38]. According to Wagner mechanism, during the solid-state reaction of corundum and periclase, the $MgAl_2O_4$ spinel phase formation takes place by the counter diffusion of the Al^{3+} and Mg^{2+} cations through the product layer, while oxygen ions remaining at the initial sites [28]. To keep the electro-neutrality, $3Mg^{2+}$ diffuse toward alumina side and $2Al^{3+}$ diffuse toward magnesia side to form 3 moles of $MgAl_2O_4$. Therefore, it is very much important to maintain shorter diffusion paths between alumina and magnesia particles in the green compact with reasonably high green density (close to 60% of the theoretical density) and reducing the median particle size of reactants to <2 μm [29,30,37,38]. In the present case, although the starting magnesia raw material had an apparently larger D_{50} (=5.63 μm), its high specific surface area (15.15 m^2/g) indicates that the primary particles are finer and the measured average size is for the agglomerates, which tend to be destroyed during ball milling. In view of these reasons, the synthesized stoichiometric MAS powder is expected to show a good sintering ability at 1650 °C as its median particle size is <2 μm and MAS phase content is >95%. Further, its compact green density is expected to be >60% of the theory as ceramic powders consolidated by aqueous colloidal gelcasting route normally show this kind of green density [32,33,35,36].

The values of solids loading and viscosities measured at a shear rate of 230 s^{-1} for MAS and alumina slurries and of green density and green porosity of consolidates and of the amount of linear shrinkage associated with each slurry upon consolidation are presented in Table 1. For an easy identification purposes, different codes are also given to these ceramics. In the sample codes, MAS stands for $MgAl_2O_4$ spinel; A for α-Al_2O_3; F for foams; the numbers 30, 35 and 40 represent the powders concentrations (vol.%) in slurries. It can be seen from this table that, MAS slurries possess relatively lower viscosities when compared with those of alumina. For example, MAS-F-35 exhibited a viscosity value of 38.4 mPa s, whereas, A-F-35 exhibited about 49.1 mPa s. The viscosity of alumina slurry was increased considerably from 49.1 to 231.2 mPa s when the alumina content in the slurry was increased from 35 to 40 vol.%. This viscosity data suggest that MAS powder was dispersed in a better manner than the alumina powder thanks to the synergistic effect of a mixture of dispersing agents (i.e., TMAH and Duramax D-3005) employed together for MAS slurries preparation. In general, MAS foams exhibited higher degrees of green porosities, hence, lower degrees of green densities in comparison to those of alumina foams. This is certainly not due to the difference existing in their corresponding specific gravities, i.e., MAS with 3.58 g/cm^3 and alumina with 3.97 g/cm^3. Both, MAS-F-30 and MAS-F-35 green foams exhibited about ∼89% porosities, and the amount of linear shrinkages associated with them were estimated to be about 7.72% and 9.27%, respectively. On the other hand, A-F-35 and A-F-40 foams exhibited porosities of about 80.74% and

Table 1
Characteristics of the MAS and alumina slurries and green bodies[a].

Sample[b]	Solids loading (vol.%)	Viscosity (mPa s)	Green density (g/cm^3)	Green porosity (%)	Shrinkage upon drying (%)
MAS-F-30	30	24.0	0.36 ± 0.01	89.81	7.71
MAS-F-35	35	38.4	0.38 ± 0.02	89.20	9.27
A-F-35	35	49.1	0.76 ± 0.02	80.74	9.05
A-F-40	40	231.2	0.48 ± 0.01	87.88	8.31

[a] Values obtained as explained in Section 2.
[b] In the sample codes, MAS stands for $MgAl_2O_4$ spinel; A for α-Al_2O_3; F for foams; the numbers 30, 35 and 40 represent the powders concentrations (vol.%) in the slurries.

87.88%, respectively. The reason for the genesis of higher porosity in MAS foams in comparison to alumina foams could be explained based on slurry characteristics such as, viscosity, homogeneity achieved in the dispersed powder particles, etc. The viscosity data reveals that MAS slurries were more homogeneous than those of alumina as the former ones exhibited lower viscosity values when the solids loading was same in both alumina and MAS slurries. Normally, the surfactant like CTMAB is known to stabilize the air/gas bubbles in the suspension [1,12]. Owing to their molecular configuration, surfactants tend to absorb onto gas-liquid interfaces with a hydrophobic part being expelled from the solvent (water) and a hydrophilic part remaining in contact with liquid. Through this mechanism, the surfactants can reduce the surface tension of the gas–liquid interfaces and hence stabilize the liquid foams for a limited period of time [1,12]. If the powder particles are not properly de-agglomerated, the liquid foam collapse, expand or shrink non-uniformly during setting in the mould leading to lower porosity and un-even distribution of pores with varied pore diameters [1,12]. The more homogeneous slurries are responsible for higher porosity achieved in MAS foams than those of alumina foams. These results are inline to those reported for alumina foams in the literature [1,12–15].

The shear rate *vs*. shear stress data of MAS-F-30 and MAS-F-35 slurries are presented in Fig. 2. It can be seen that both the suspensions exhibited, in general, a shear thinning behavior over the whole shear rate range tested with some exceptions at higher shear rates. The un-dissolved monomer particles and the un-broken powder agglomerates (during 24 h milling in polypropylene bottles) could be responsible for the observed slight shear thickening behavior at some shear rates tested (Fig. 2). However, at the end of the shear rate range tested, both suspensions showed again the shear thinning behavior. Normally, the higher shear rates destroy powder agglomerates leading to shear thinning of the suspension, what has been observed in the present case too. The reason for not braking of the powder agglomerates during milling in polypropylene

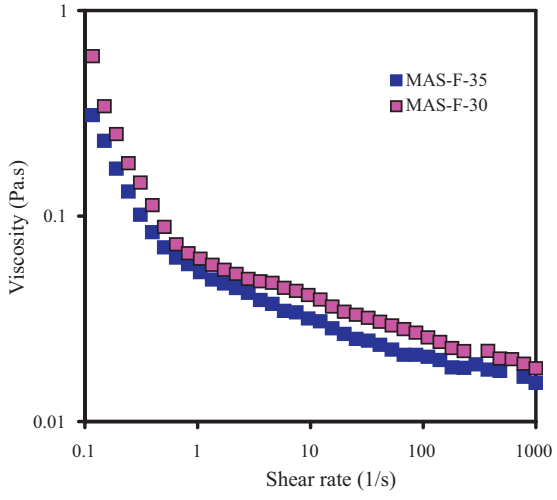

Fig. 2. Viscosity *vs*. shear rate of MAS-F-30 and MAS-F-35 slurries (please see Table 1 for other details).

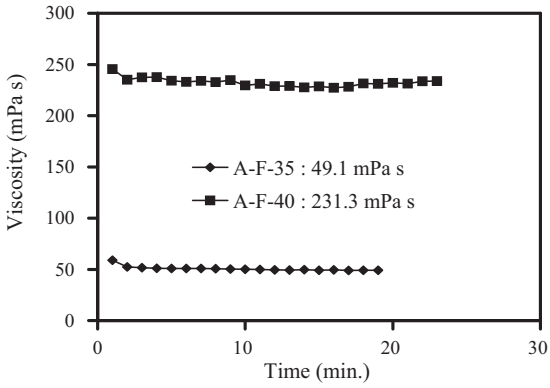

Fig. 3. The change in absolute viscosity of A-F-35 and A-F-40 slurries as a function of measured time in a piston type viscometer (please see Table 1 for other details).

bottles containing alumina balls (ball to powder ratio of 3:1) even after for 24 h time could to be attributed to the lower solids loading of the slurries (Table 1). The effective deagglomeration was reported for the suspensions containing >45 vol.% MAS powder solids loading [32,33,36]. Thus, higher solids loaded slurries are not only important for fabricating the near-net shape components but also to fabricate ceramic components with minimal defects at micro-structural levels [36]. Fig. 3 presents the viscosity behavior of A-F-35 and A-F-40 slurries under constant shear rate in a piston type viscometer as a function of time. A quite stability in viscosities of these slurries over 20 min of constant shear rate is seen. It indicates that both alumina slurries show a near Newtonian behavior.

Properties of MAS (solid, MAS-S and foams, MAS-F-30 & MAS-F-35;) and alumina (solid, A-S and foams, A-F-35 & A-F-40;) solids and foams sintered for 1 h at 1650 °C and for 2 h at 1600 °C, respectively, are presented in Table 2 along with the codes given to them. Codes are same as given in Table 1, where S stands for solid bodies. MAS-S had a green density of 1.92 g/cm^3 (i.e., 53.63% of TD), whereas, A-S had about 2.05 g/cm^3 (51.63% of TD). It can be seen from these sintered properties that, in general, alumina underwent higher densification when compared to MAS powder as the former one had a finer particle size (1.84 μm) than MAS, which had about 1.91 μm. As far as, the effect of structure of consolidate (i.e., foam or solid) on densification behavior is concerned, despite their relatively higher thermal mass, the solid bodies (i.e., MAS-S and A-S with about 10 grams mass and about 8 mm thickness) underwent higher densification when compared to their corresponding foam structures, which had very fine webs. This anomalous behavior could be attributed to the degree of compactness achieved in green foam or solid bodies. This sintered data suggests that the webs of green foams had lower degrees of compactness among powder particles in comparison to those solid pellets uni-axially pressed in a metal die under a pressure of about 200 MPa. Interestingly and as expected, the trends noted in apparent porosity and water absorption capacity values are in agreement with the one noted in relative density values. As far as bulk properties including total porosity (i.e., theoretical porosity), compressive strength, pore diameter and total linear shrinkage upon sintering are concerned, MAS

Table 2
Properties of MAS and alumina (A) porous and solid bodies sintered at 1600-1650 °C for 1-2 h[a].

Sample[b]	Sintering temp. (°C) and soaking time (h)	Web properties				Bulk properties			
		Bulk density (g/cm^3)	Relative density (%)	Apparent porosity (%)	Water absorption capacity (%)	Total porosity (%)	Compressive Strength (MPa)	Pore diameter (μm)[c]	Total-linear shrinkage (%) upon sintering
MAS-F-30	1650/1	3.32 ± 0.02	92.73	0.04	0.01	76.73	5.11 ± 2.02	55–310	33.03
MAS-F-35	1650/1	3.38 ± 0.01	94.41	0.32	0.09	74.85	5.24 ± 1.96	50–300	33.44
A-F-35	1600/2	3.87 ± 0.02	97.48	0.12	0.06	67.05	32.55 ± 2.2	192–965	38.83
A-F-40	1600/2	3.90 ± 0.02	98.26	0.32	0.01	72.13	27.32 ± 2.8	170–930	39.77
MAS-S	1650/1	3.43 ± 0.02	95.81	0.01	0.01	–	–	–	14.21
A-S	1600/2	3.93 ± 0.01	98.99	0.93	0.28	–	–	–	14.99

[a] Values obtained as explained in Section 2.
[b] Codes are same as given in Table 1 and S stands for solid bodies.
[c] Arrived based on SEM investigations.

foams exhibited the higher values of total porosity (74.85–76.73%) and the lower values of total linear shrinkage (33.03–33.44%), compressive strength (5.11–5.24 MPa) and pore diameters range (50–310 μm), whereas, the alumina foams exhibited the higher total linear shrinkage (38.83–39.77%), compressive strength (27.32–32.55 MPa) and pore diameter range (192–930 μm) values and the lower total porosity (67.05–72.13%) values. The total linear shrinkage values measured for MAS-S (14.21%) and A-S (14.99%) match very well with those reported for MAS and alumina solid bodies in the literature [30,40,41]. In line to the sintered properties of webs, their bulk properties of foams were also found to be strongly influenced by their slurry characteristics. Good characteristics of MAS slurries were responsible for generating higher porosity and pore diameter with much narrow distribution in MAS foams in comparison to alumina foams. Though the alumina foams exhibited higher compressive strengths (>27 MPa), they exhibited catastrophic failure under compression with much low energy absorption capabilities, whereas, it is completely different story in the case of MAS foams. These latter foams exhibited only about 5 MPa compressive strength but they did not exhibit catastrophic failure. The more uniform distribution of pores with relatively narrow pore size distribution could be responsible for such behavior under compression for MAS foams. Foams with this kind of behavior are highly recommended for energy absorption applications [33,35].

The fracture SEM micrographs of MAS-F-35 (sintered at 1650 °C for 1 h) with (a) 375 μm; (b) 150 μm and (c) 30 μm magnifications are presented in Fig. 4(a–c), respectively. The bi-model type pores can be seen from these micrographs, some pores with diameters as small as 50 μm and some with as high as >300 μm. A close look at these micrographs reveals that all the large pores are inter-connected through small pores. Fig. 4(c) reveals the presence of closely packed equi-axed/spherical grains in the sintered webs of MAS-F-35 foam substantiating the determined values of bulk density, apparent porosity and water absorption capacity. In contrary to these, pores with about 200 μm to 1 mm diameters can be seen in alumina, A-F-40, foam sintered at 1600 °C for 2 h (Fig. 5). Similar types of pores were observed for alumina gelcast foams prepared by Sepulveda and her team [1,12]. Thus, the porosity and pore size distributions of these sintered foams are comparable with those reported for other ceramic foams in literature [1,12,17].

Typical stress–strain profiles generated by the compression of MAS-F-35 foam (three numbers made from MAS-F-35 suspension) sintered at 1650 °C for 1 h are presented in Fig. 6. It is seen that these foams exhibited compressive strengths of about 4–6.3 MPa with a continuous energy absorption tendency for quite long strains (>0.4 mm/mm). Normally, foams show three different characteristic regions namely *linear elastic region*, *plateau* and *densification* in stress–strain curves under compression [11,12,17]. *Linear elastic region* is the initial portion of the curve, where elastic deformation of the cell wall materials takes place. Beyond a *critical stress*, cells begin to collapse at a roughly constant stress, known as *plateau stress*. Ultimately, at high strains, the flow stress increases rapidly, known as *densification*. Normally, this type of behaviour is absent in the case of ceramic foams, where collapse of foams occurs by brittle fracture of cell walls and the structure fractures macroscopically. Therefore, no contact of the opposite cell wall with that of the compression anvil and no *densification* process. Interestingly, MAS-F-35 foams exhibited (Fig. 6) a different fracture mechanism, which is normally seen in the case of honeycomb structures, but not in ceramic foam structures [17]. This is due to fact that honeycomb structure contains regular array of channels with uniform distance between the cell walls and the similar thickness for all cell walls and similar strength hence continuous energy absorption under compression, which is totally absent in foam structures. Despite this, what can be observed from Fig. 6 is after a critical stress, a slight brittle fracture of cells followed by a constant densification mechanism. Foams with this kind of behavior are highly preferred for applications where high (impact) energy needs to be absorbed [12,17]. The measured compressive strength of about 4–6.3 MPa for MAS-F-35 foam is in fact a higher value for any normal ceramic foam having a porosity of >75% with uniform pore size distribution. These results indicate high prospects for MAS foams in applications where high energy absorption is needed [17]. Alumino-silicate composition based reticulated foams having 30 pores per linear inch (PPI) supplied

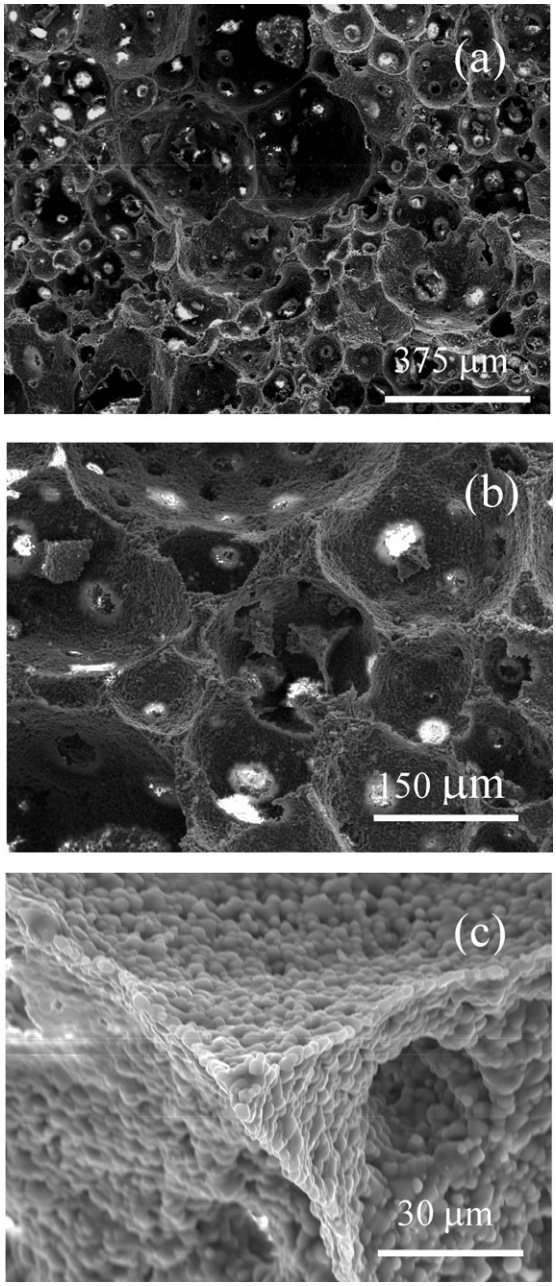

Fig. 4. The SEM micrographs of MAS-F-35 foam sintered at 1650 °C for 1 h recorded with (a) 375 µm; (b) 150 µm and (c) 30 µm scale magnifications.

by Belarussian State Research Production Concern of Powder Metallurgy and New Materials (BPMC), Belarus, exhibited a compression strength of about 2 MPa. This same reticulated foam after encapsulation with a rubber of about 1 mm thickness exhibited strength of about 2.5 MPa [17]. When compared with these reticulated foams, the MAS foams prepared in this study exhibited considerably higher compressive strengths. On the other hand, alumina foams exhibited very high compressive strengths (27.32–32.55 MPa) but broke down catastrophically under compression load (Fig. 7). Foams, A-F-35 and A-F-40 exhibited compressive strength values of about 32.55 ± 2.2 and 27.32 ± 2.8 MPa, respectively, after sintering for 2 h at 1600 °C. The stress-strain profiles of these alumina foams clearly indicate

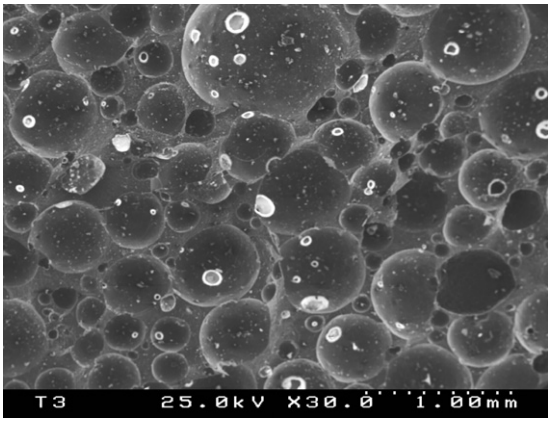

Fig. 5. A typical SEM micrograph of A-F-40 sintered at 1600 °C for 2 h.

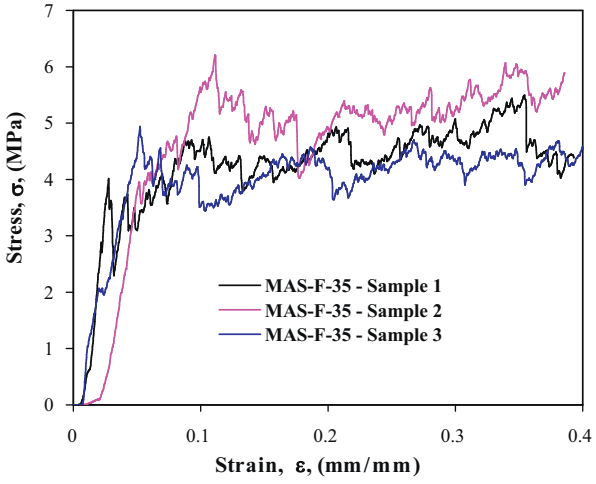

Fig. 6. Typical stress–strain profiles generated upon compression of MAS-F-35 foams sintered for 1 h at 1650 °C.

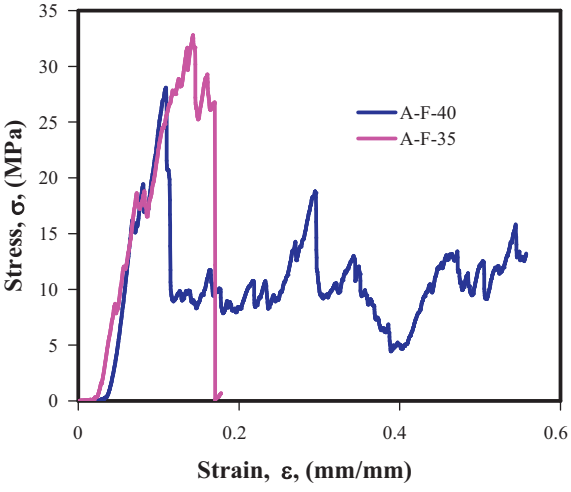

Fig. 7. Typical stress–strain curves of A-F-35 and A-F-40 foams sintered for 2 h at 1600 °C.

that though these foams possesses high compressive strengths they fracture catastrophically before achieving even a strain of about 0.2 with the complete absence of *plateau* and *densification* processes. Nevertheless, these results are inline to those of alumina foams reported in the literature [1,12–15].

4. Conclusions

The following conclusions can be drawn from this study: A magnesium aluminate spinel (MAS) powder with more than 98% spinel phase could be prepared by calcining a stoichiometric mixture of alumina and calcined caustic magnesia for 1 h at 1400 °C after compacting by following temperature induced gelation (TIG) process. The surface of the MAS powder can be passivated against hydrolysis by treating in ethanol solution containing H_3PO_4 and $Al(H_2PO_4)_3$ for 24 h at 80 °C. The surface treated MAS powder could be dispersed in aqueous media to achieve stable suspensions with 30–35 vol.% solids loading using suitable amounts of TMAH and Duramax D-3005 as dispersing agents. MAS foams with about 74–76% porosity and about 4–7.2 MPa compressive strength can be prepared following gelcasting of aqueous suspensions in which foam can be created by adding aqueous solution of CTMAB foaming agent followed by consolidation, drying and sintering for 1 h at 1650 °C. Alumina foams prepared following same aqueous gelcasting route exhibited compressive strength values of as high as 27–32 MPa with a porosity in the range of 67–72%. The commercial alumina (CT-3000SG, Alcoa-Chemie GmbH, Ludwigshafen, Germany) powder exhibited higher sintering ability than that of stoichiometric MAS powder synthesized in this study following a conventional solid-state reaction from alumina and magnesia powders compacts, when sintered at 1600 °C for 2 h and 1650 °C for 1 h, respectively.

Acknowledgements

Author thanks Dr. G. Sundararajan, Director, ARCI for his kind encouragement for publishing this paper. He also expresses his gratitude to his colleagues at ARCI for their kind contributions to this study. Further, he thanks Prof. J.M.F. Ferreira and Dr. S.M. Olhero, Department of Ceramics and Glass Engineering, CICECO, University of Aveiro, Aveiro, P-3810193, Portugal for their valuable technical discussions during this study.

References

[1] P. Sepulveda, Gelcasting foams for porous ceramics, Bull. Am. Ceram. Soc. 76 (10) (1997) 61–65, and references therein.
[2] X. Zhu, D. Jiang, S. Tan, The control of slurry rheology in the processing of reticulated porous ceramics, Mater. Res. Bull. 37 (3) (2002) 541–553.
[3] S. Kwon, G. Son, J. Suh, K.T. Kim, Densification and grain growth of porous alumina compacts, J. Am. Ceram. Soc. 77 (12) (1994) 3137–3141.
[4] S. Geis, J. Fricke, P. Ľobmann, Electrical properties of PZT aerogels, J. Eur. Ceram. Soc. 22 (7) (2002) 1155–1161.
[5] H.X. Peng, Z. Fan, J.R.G. Evans, J.J.C. Busfield, Microstructure of ceramic foams, J. Eur. Ceram. Soc. 20 (7) (2000) 807–813.
[6] M. Takahashi, T. Mizuno, Y. Shiroki, T. Yokoyama, H. Abe, M. Naito, Porous alumina with a double-layered structure fabricated by pore-controlled in situ solidification, in: S. Hirano, G.L. Messing, N. Claussen (Eds.), Ceramic Powder Science VI, Ceramic Transactions, vol. 112, American Ceramic Society, Westerville, OH, 2001, pp. 559–564.
[7] S. Izuhara, K. Kawasumi, M. Yasuda, H. Suzuki, M. Takahashi, Highly porous cordierite ceramics fabricated by in situ solidification, in: S. Hirano, G.L. Messing, N. Claussen (Eds.), Ceramic Powder Science VI, Ceramic Transactions, vol. 112, American Ceramic Society, Westerville, OH, 2001, pp. 553–558.
[8] K. Jono, M. Fuji, M. Takahashi, Porous ceramics for building materials fabricated by *in situ* solidification method using natural polymer and waste resources, J. Ceram. Soc. Jpn. 112 (5) (2004) S138–S143.
[9] K. Adachi, M. Fuji, M. Takahashi, Fabrication of porous construction ceramics by gelcasting of waste resources, in: K.A. Khor, Y. Watanade, K. Komeya, H. Kimura (Eds.), Materials Processing for Properties and Performance (MP3), vol. 2, Institute of Materials East Asia, 2004, pp. 219–225.
[10] J.S. Woyansky, C.E. Scott, W.P. Minnear, Processing of porous ceramics, Am. Ceram. Soc. Bull. 71 (11) (1992) 1674–1682.
[11] L.J. Gibson, M.F. Ashby, Cellular Solids: Structure and Properties, Pergamon Press, Oxford, U.K, 1988, pp. 1-10.
[12] P. Sepulveda, J.G.P. Binner, Processing of cellular ceramics by foaming and in situ polymerization of organic monomers, J. Eur. Ceram. Soc. 19 (12) (1999) 2059–2066.
[13] J.S. Ha, Effect of atmosphere type on the gelcasting behavior of Al_2O_3 and evaluation of green strength, Ceram. Int. 26 (3) (2000) 251–254.
[14] O. Lyckfeldt, J.M.F. Ferreira, Processing of porous ceramics by starch consolidation, J. Eur. Ceram. Soc. 18 (2) (1998) 131–140.
[15] S. Dhara, P. Bhargava, A simple direct casting route to ceramic foams, J. Am. Ceram. Soc. 86 (10) (2003) 1645–1650.
[16] I. Ganesh, D.C. Jana, S. Shaik, N. Thiyagarajan, An aqueous gelcasting process for sintered silicon carbide ceramics, J. Am. Ceram. Soc. 89 (10) (2006) 3056–3064.
[17] V. Jain, R. Johnson, I. Ganesh, B.P. Saha, Y.R. Mahajan, Effect of rubber encapsulation on the comparative mechanical behavior of ceramic honeycomb and foam, Mater. Sci. Eng. A347 (2003) 109–122.
[18] C. Baudin, R. Martinez, P. Pena, High-temperature mechanical behavior of stoichiometric magnesium spinel, J. Am. Ceram. Soc. 78 (7) (1995) 857–1862.
[19] J.H. Belding, E.A. Letzgus, Process for producing magnesium aluminate spinel, U.S. Patent No. 3 950 504, 13 April, 1976.
[20] K.E. Green, J.L. Hastert, D.W. Roy, Polycrystalline $MgAl_2O_4$ spinel – a broad band optical material for offensive environments, in Window & Dome rial, Proc. Soc. Photo-Opt. Instrum. Eng. A90-34551 (1989) 14–74.
[21] S. Angappan, L.J. Berchmans, C.O. Augustin, Sintering behaviour of $MgAl_2O_4$ – a prospective anode material, Mater. Lett. 58 (2004) 2283–2289.
[22] Y. Shimizu, H. Arai, T. Seiyama, Theoretical studies on the impedance-humidity characteristics of ceramic humidity sensors, Sens. Actuators 7 (1985) 11–22.
[23] Y. Urita, K. Yamaguchi, I. Takita, K. Furuta, Y. Natsuo, Properties of alumina–magnesia refractories for steel ladles, Taika-butsu 45 (11) (1993) 664–672.
[24] M. O'Driscoll, Fused Spinel – Monolithics Market Future, IM Fused Minerals Review, Special Issue, (1997) 36–46.
[25] I. Ganesh, S. Bhattacharjee, B.P. Saha, R. Johnson, K. Rajeshwari, R. Sengupta, M.V. Ramanarao, Y.R. Mahajan, An efficient $MgAl_2O_4$ spinel additive for improved slag erosion and penetration resistance of high-Al_2O_3 and MgO-C refractories, Ceram. Inter. 28 (2002) 245–253.
[26] A. Le Valant, A. Garron, N. Bion, F. Epron, D. Duprez, Hydrogen production from raw bioethanol over $Rh/MgAl_2O_4$ catalyst Impact of impurities: heavy alcohol, aldehyde, ester, acid and amine, Catal. Today 138 (3–4) (2008) 169–174.
[27] O.R. Evans, A.T. Bell, T.D. Tilley, Oxidative dehydrogenation of propane over vanadia-based catalysts supported on high-surface-area mesoporous $MgAl_2O_4$, J. Catal. 226 (2) (2004) 292–300.
[28] Z.E. Nakagawa, N. Enomoto, I.S. Yi, K. Asano, Effect of corundum/periclase sizes on the expansion behavior during synthesis of spinel, in: Proc. UNITECER'95, Congress, Tokyo, (1995), pp. 379–386.
[29] I. Ganesh, K.A. Teja, N. Thiyagarajan, R. Johnson, B.M. Reddy, Formation and densification behavior of magnesium aluminate spinel: the influence of CaO and moisture in the precursors, J. Am. Ceram. Soc. 88 (10) (2005) 2752–2761.

[30] I. Ganesh, S.M. Olhero, A.H. Rebelo, J.M.F. Ferreira, Formation and densification behaviour of $MgAl_2O_4$ spinel: the influence of processing parameters, J. Am. Ceram. Soc. 91 (6) (2008) 1905–1911.
[31] L. Kaiqi, P. Wei, F. Zhengkun, L. Yongfeng, W. Bingjun, Gelcasting of alumina-spinel refractories, Key Eng. Mater. 368–372 (2008) 1149–1151.
[32] I. Ganesh, Near-net shape β-$Si_4Al_2O_2N_6$ parts by hydrolysis induced aqueous gelcasting process, Inter. J. Appl. Ceram. Tech. 6 (1) (2009) 89–101.
[33] I. Ganesh, S.M. Olhero, P.M.C. Torres, J.M.F. Ferreira, Gelcasting of $MgAl_2O_4$ spinel powder, J. Am. Ceram. Soc. 92 (2) (2009) 350–357.
[34] L. Bergström, Method for forming ceramic powders by temperature induced flocculation, U.S. Patent 5,340,532, 23rd August, 1994.
[35] S.M. Olhero, I. Ganesh, P.M.C. Torres, J.M.F. Ferreira, Surface passivation of $MgAl_2O_4$ spinel powder by chemisorbing H_3PO_4 for an easy aqueous processing, Langmuir 24 (17) (2008) 9525–9530.
[36] M.A. Janney, S.D. Nunn, C.A. Walls, O.O. Omatete, R.B. Ogle, G.H. Kirby, A.D. McMillan, Gelcasting, in: M.N. Rahman (Ed.), The Handbook of Ceramic Engineering, Marcel Dekker, New York, 1998, , pp. 1–15, and references there in.
[37] I. Ganesh, S. Bhattacharjee, B.P. Saha, R. Johnson, Y.R. Mahajan, A new sintering aid for magnesium aluminate spinel, Ceram. Inter. 27 (2001) 773–779.
[38] I. Ganesh, B. Srinivas, R. Johnson, B.P. Saha, Y.R. Mahajan, Microwave assisted solid state reaction synthesis of $MgAl_2O_4$ spinel powders, J. Euro. Ceram. Soc. 24 (2004) 201–207.
[39] B.D. Cullity, Elements of XRD, 2nd ed., Addison-Wesley, Reading, MA, 1978.
[40] I. Ganesh, G. Sundararajan, S.M. Olhero, P.M.C. Torres, J.M.F. Ferreira, A novel colloidal processing route to alumina ceramics, Ceram. Inter. 36 (2010) 1357–1364.
[41] I. Ganesh, P.M.C. Torres, J.M.F. Ferreira, Densification behavior of combustion derived Al_2O_3 powders, Ceram. Inter. 35 (2009) 1173–1179.